

Simple theory for the electronic and atomic structure of small clusters

D. Tománek and S. Mukherjee

*Institut für Theoretische Physik, Freie Universität Berlin, Arnimallee 14,
D-1000 Berlin 33, West Germany*

K. H. Bennemann*

*Institut für Theoretische Physik, Eidgenössische Technische Hochschule Zürich,
CH-8093 Zürich, Switzerland*

(Received 22 October 1982; revised manuscript received 24 February 1983)

A simple theory is presented for various fundamental properties of small clusters. In particular, we calculate the cohesion, the magic numbers, bond contraction, stability of atomic structures, and alloy formation as a function of cluster size, and determine also the Coulomb explosion of small multiply charged clusters.

I. INTRODUCTION

Recently, clusters of a few to several hundred atoms have been studied intensively.¹⁻¹² It has been observed that such clusters possess many interesting properties: for example, with regard to atomic and electronic structure,⁴⁻¹¹ catalysis,^{13,14} and absorption of electromagnetic energy.³ It is the main purpose of this paper to explain some interesting properties of small clusters such as cohesive energy, atomic bond contraction, crystal-structure stability, alloy formation, and stability of electrically charged clusters by using a simple theory. This permits a transparent physical understanding of the atomic and electronic structure as a function of cluster size and application to various other problems concerning small clusters. Furthermore, the simple theory presented here can be used as a first orientation for understanding new experimental results.

In Sec. II we outline the calculation of various properties as a function of cluster size and present results. In Sec. III we present a discussion of our results and a summary.

II. CALCULATION OF VARIOUS PROPERTIES OF SMALL CLUSTERS

In the following we present a simple electronic theory for calculating various properties as a function of cluster size. In order to understand the atomic structure, magic numbers,¹ Coulomb explosion of electrically charged clusters,² catalytic activity, etc., the binding energy of an atom in a metallic cluster needs to be determined.

A. Cohesive energy

The binding energy $E_{\text{coh}}(i)$ of an atom i can be quite generally expressed by the bulk cohesive energy $E_{\text{coh}}(\text{bulk})$ as follows:

$$E_{\text{coh}}(i) = (Z_i/Z_b)^{1/2} E_{\text{coh}}(\text{bulk}) + E_R. \quad (2.1)$$

Here, Z_i and Z_b are the effective atomic coordination numbers of the atom i and a bulk atom, respectively. As we show in the Appendix by using the moment expansion technique for the electronic density of states, Eq. (2.1) can be used not only for calculating cohesion due to d elec-

trons, but also for calculating cohesion in s - p -electron metals. While it is known that for transition metals Z_i can be approximated by the nearest-neighbor coordination number Z_i^1 , this will also be the case provided that for the n th neighbor $Z_i^n/Z_i^1 = \text{const}$ throughout the cluster, which is a physically reasonable assumption. Also, Eq. (2.1) can account approximately for local charge neutrality.

Note, in Eq. (2.1) the energy E_R due to repulsive interactions can be replaced by a hard-core potential and neglected at equilibrium distances for calculating cohesion, structural stability, etc. It is well known that one has to consider E_R in Eq. (2.1) only for determining deviations from the interatomic equilibrium distances, as will be the case in Sec. II C.

The average cohesive energy in a cluster with N atoms is

$$\langle E_{\text{coh}} \rangle = \frac{1}{N} \sum_i E_{\text{coh}}(i), \quad (2.2)$$

where i sums over all cluster atoms. Similarly, the average bond energy in a cluster with N_b bonds is given by

$$\langle E_{\text{bond}} \rangle = \frac{1}{N_b} \sum_i E_{\text{coh}}(i). \quad (2.3)$$

These relatively simple formulas can now be used to study how the bond energy varies with cluster size and to determine the magic numbers of atoms for which small clusters are particularly stable. In our calculation, atomic shells are numbered in the cluster according to the minimum number of hops necessary to get from the central atom to any atom in the considered cluster shell. In Fig. 1(a) we present results for $\langle E_{\text{coh}} \rangle$ and $\langle E_{\text{bond}} \rangle$ as a function of cluster size for clusters with fcc structure.¹⁵ These results compare very well with the observed melting temperature for small Au clusters of different size.¹⁶

In Fig. 1(b) we show results for the binding energy of the most loosely bound cluster atom as a function of N . Clearly, such clusters are particularly stable for which the smallest $E_{\text{coh}}(i)$ decreases sharply upon adding another atom. Thus one is tempted to conclude from Fig. 1(b) that clusters with the magic numbers 13, 19, 55, etc., are particularly stable. Note, the magic numbers 13, 55, ... for icosahedra clusters with complete outermost atomic shells have been explained previously by geometric arguments.¹ For the incomplete outermost cluster shell we calculated

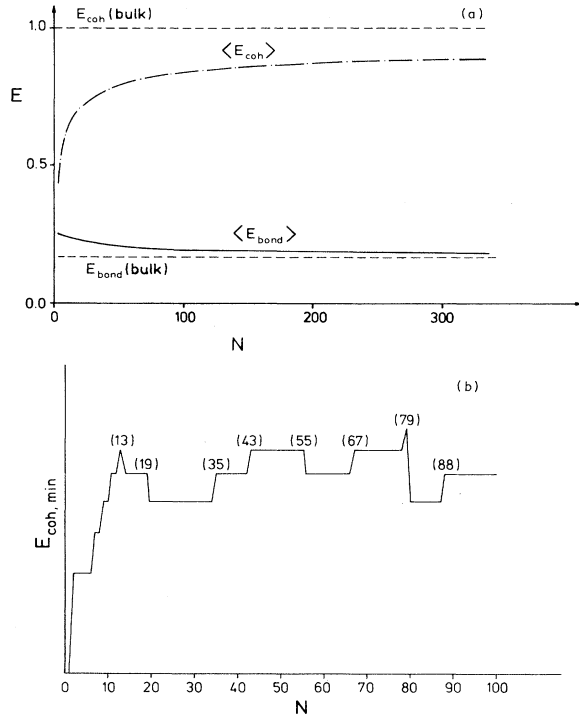


FIG. 1. (a) $\langle E_{\text{coh}} \rangle$ and $\langle E_{\text{bond}} \rangle$ for fcc clusters using Eqs. (2.2) and (2.3). (b) Smallest binding energy $E_{\text{coh},\text{min}}$ for a cluster atom as a function of the total number N of cluster atoms. Construction of the clusters is described in Sec. III.

the smallest $E_{\text{coh}}(i)$ as a function of N by adding atoms always next to the atoms already present in the incomplete shell.

B. Structural stability

Owing to the small portion of surface atoms in extremely large clusters, the surface energy has a negligible effect on their crystalline atomic structure. As the cluster size decreases the surface energy gets more and more important and might change the atomic structure of the cluster to one with lower surface energy. This has been observed⁴ for Nb, Mo, W, and Ta clusters with bulk bcc structure. Therefore, we investigate in the following the transition from fcc structure for small clusters to bcc structure for large clusters.

Clearly, the total cohesive energy of a cluster can be written in terms of the average binding energy $E_{\text{coh},b(s)}(i)$ per atom as

$$E_{\text{coh}} = (N - N_s)E_{\text{coh},b} + N_s E_{\text{coh},s}. \quad (2.4)$$

Here, b and s refer to bulk and surface, respectively. N_s is the number of surface atoms. Surface atoms are defined as those with a coordination number smaller than 10, in analogy to close-packed metal surfaces.

The cohesive energy difference for a bcc and fcc cluster is given by

$$\begin{aligned} E_{\text{coh}}(\text{fcc}) - E_{\text{coh}}(\text{bcc}) &= (N - N_s)[E_{\text{coh},b}(\text{fcc}) - E_{\text{coh},b}(\text{bcc})] \\ &\quad + N_s[E_{\text{coh},s}(\text{fcc}) - E_{\text{coh},s}(\text{bcc})]. \end{aligned} \quad (2.5)$$

Here, we used the fact that the dispersion N_s/N is the same for fcc and bcc clusters as suggested by Fig. 2. The structural transition occurs when

$$E_{\text{coh}}(\text{fcc}) - E_{\text{coh}}(\text{bcc}) = 0.$$

In Eq. (2.5) the surface energies can be approximately written as

$$N_s(E_{\text{coh},s} - E_{\text{coh},b}) = E_{\text{coh},b} \sum_{i=1}^{N_s} [(Z_i/Z_b)^{1/2} - 1]. \quad (2.6)$$

As discussed in the Appendix, second-nearest-neighbor interactions may be accounted for by using the effective coordination number $Z_i = Z_i^1 + aZ_i^2$, where Z_i^1 and Z_i^2 refer to nearest neighbor (NN) and next-nearest neighbor (NNN), respectively. The parameter a is determined from the distance dependence of the electron hopping integral. For the case of binding due to d electrons we use the value $a_{\text{fcc}} = 0.08$ and $a_{\text{bcc}} = 0.4$ (see the Appendix for details).

Since the change in the cohesive energy resulting from a transition from fcc to bcc is at least 1 order of magnitude lower than the cohesive energy itself, we divide Eq. (2.6) by $NE_{\text{coh},b}$ and obtain as a condition for the structural transition

$$\begin{aligned} \frac{E_{\text{coh},b}(\text{bcc}) - E_{\text{coh},b}(\text{fcc})}{E_{\text{coh},b}} &= \frac{1}{N} \left[\sum_{i=1}^{N_s} [(Z_i/Z_b)^{1/2} - 1]_{\text{fcc}} - \sum_{i=1}^{N_s} [(Z_i/Z_b)^{1/2} - 1]_{\text{bcc}} \right]. \end{aligned} \quad (2.7)$$

The expression on the left-hand side is a constant, which for large clusters depends on the bulk electronic properties of the material only. Values for this are given in Table I for different bcc materials. The expression on the right-hand side depends only on the cluster geometry and is given as a universal curve in Fig. 3. Note, Eq. (2.7)

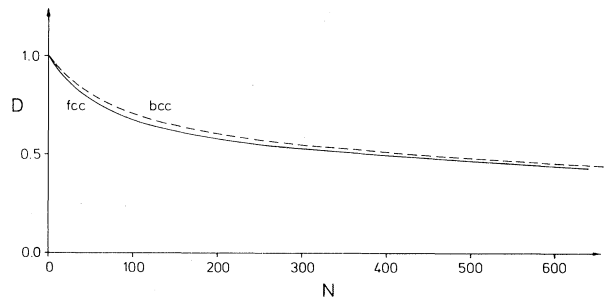


FIG. 2. Dispersion $D = N_s/N$ for fcc- and bcc-type clusters to illustrate that $N_s(\text{bcc}) \approx N_s(\text{fcc})$.

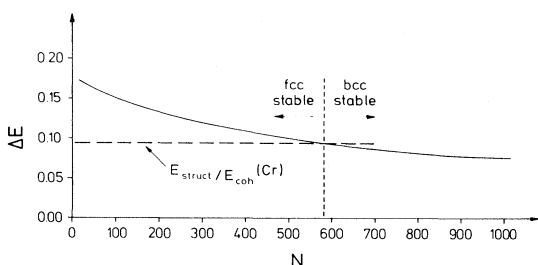


FIG. 3. Graphical determination of structural stability in small bcc clusters. Solid curve is the relative structure energy of clusters which is defined by the right-hand side of Eq. (2.7). The dashed curve is the value $[E_{\text{struct},b(\text{bcc})} - E_{\text{coh},b(\text{fcc})}] / E_{\text{coh},b}$ for Cr.

presents a relatively simple expression determining the structural stability of metallic clusters. Its validity is essentially based on the applicability of Eq. (2.1).

As an illustration we study in Fig. 3 the structural stability of Cr clusters. The transition from close-packed to bulk bcc structure is expected to occur for a cluster size of about 580 atoms. Note, a similar transformation from

$$E_{\text{coh}}(i) = \frac{E_{\text{coh}}(\text{bulk})}{(1-q/p)(Z_{\text{bulk}})^{1/2}} \left[\left(\sum_j \exp[-2q(R_j/R_0 - 1)] \right)^{1/2} - \frac{1}{(Z_i)^{1/2}} \frac{q}{p} \sum_j \exp[-p(R_j/R_0 - 1)] \right] \quad (2.8)$$

given in the Appendix [see Eq. (A7)]. Here, R_0 and R_j are the nearest-neighbor distances before and after relaxation, respectively, and p and q are parameters. In this formula, a repulsive interaction term E_R mainly due to s -electron density compression has been included explicitly in addition to the binding term in Eq. (2.1). As discussed later, this repulsion was not necessary to include for determining $\langle E_{\text{coh}} \rangle$, the structure stability, etc. The equilibrium interatomic distance is then obtained from

$$\frac{\partial E_{\text{coh}}(i)}{\partial \bar{r}_i} = 0. \quad (2.9)$$

From Eqs. (2.8) and (2.9) the contraction may be calculated for all cluster shells. However, for simplicity the cluster contraction is now approximately determined by taking

icosahedra to cuboctahedra structure, which was observed in small Pd, Pt, and Au clusters,⁵ has already been studied previously¹⁰ and could also be determined by using Eq. (2.7).

C. Average atomic-distance contraction

Recently, it has been observed that in small metallic clusters such as Cu, Ni, and Pt the average interatomic distance is smaller than in the corresponding bulk crystals.^{6,7} One reason for this contraction is the surface pressure.¹² This causes the (intershell) distances in the cluster to decrease homogeneously by less than 0.5% in small clusters of 50 atoms or somewhat larger. However, still a larger effect is expected due to an inhomogeneous contraction mainly for the surface shells of the cluster. This contraction results from the unsaturated bonds of the surface atoms, similar to planar metal surfaces. Note, this assumption of a contraction mainly confined to the surface has been found essential for the analysis of lattice vibrations in small particles.¹⁹

In order to calculate the atomic-distance contraction as a function of cluster size, we use for the cohesive energy the expression

into account only the decrease in the distance between the surface shell and the next shell. All other interatomic distances are kept at the bulk value. Then the average distance between the atomic shells is given by

$$\langle r \rangle = n^{-1} [n_1 r_1 + (n - n_1) r_0], \quad (2.10)$$

where r_0 and r_1 are the distances between the shells in the bulk and at the surface, respectively. n_1 is the number of bonds between the surface and second shell and n is the total number of bonds.

In Fig. 4 we show results for the average bond contraction $\Delta R = (\langle r \rangle - r_0) / r_0$ as a function of the total number of cluster atoms. By comparison with experiment it should be possible to check our essential assumption that the cluster contraction is mainly due to the surface layers.

TABLE I. Values for the structure energy $E_{bs} = E_{\text{coh}}(\text{bcc}) - E_{\text{coh}}(\text{fcc})$, the bulk cohesive energy $E_{\text{coh},b}$, and their ratio for different bcc metals. Also included is the critical cluster size N_{crit} , at which the structure transformation is expected from Eq. (2.7).

	ΔE_{bs}^a (eV)	$E_{\text{coh},b}^b$ (eV)	$\Delta E_{bs} / E_{\text{coh},b}$	N_{crit}
V	0.286	5.33	5.37×10^{-2}	2950
Cr	0.381	4.12	9.25×10^{-2}	580
Nb	0.286	7.48	3.82×10^{-2}	8190
Mo	0.381	6.83	5.58×10^{-2}	2630
Ta	0.286	8.11	3.53×10^{-2}	10380
W	0.381	8.81	4.32×10^{-2}	5660

^aReference 17, Fig. 2.

^bReference 18.

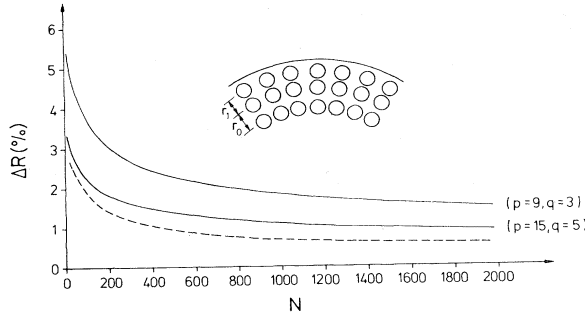


FIG. 4. Average bond contraction ΔR in fcc clusters for different choice of parameters p, q (solid line). Also included are previous results by Gordon *et al.* (Ref. 10) for $p=15, q=5$ (dashed line).

D. Segregation in alloy clusters

To learn about the important problem of alloy formation in small clusters, it is of particular interest to study the effect of the cluster size on the segregation behavior in alloy clusters. Note, drastic changes in the catalytic activity for ethane hydrogenolysis have been found in CuRu clusters of identical composition but different size,¹⁴ which have been blamed on differences in the surface composition.

In order to calculate this surface composition, the free energy has to be minimized. This yields²⁰

$$\frac{x_s}{1-x_s} = \frac{x_b}{1-x_b} e^{-\Delta E/kT}, \quad (2.11)$$

where x_s denotes the surface concentration of A in the alloy $A_x B_{1-x}$ and ΔE the heat of segregation. In general, one expects the atoms with the lower surface energy to segregate to the surface. For bulk alloys $A_x B_{1-x}$ with strong surface segregation we expect strong demixing in the case of corresponding small clusters. Note that for small clusters the bulk concentration x_b of A depends appreciably on x_s . Then, the number $N_{A,s}$ of A atoms at the surface of an N -atom cluster containing totally N_A A atoms is given by

$$\frac{N_{A,s}}{N_s - N_{A,s}} = \frac{N_A - N_{A,s}}{(N - N_s) - (N_A - N_{A,s})} e^{-\Delta E/kT}. \quad (2.12)$$

Note, Eq. (2.12) can be easily extended to determine $N_{A,s}^i$, where i refers to the first, second, etc., surface shell with coordination number different from bulk.

In our case the heat of segregation is the difference of surface energies for A and B atoms. For transition metals, within the tight-binding approximation, and using Eq. (A2), one obtains the expression²¹

$$\Delta E = (W_{AB}/20)[1 - (Z_s/Z_b)^{1/2}](n_A - n_B) \times (10 - n_A - n_B). \quad (2.13)$$

Here,

$$W_{AB} = [1 + (\Delta C/W)^2]W.$$

In this expression ΔC is the relative position of the bands of A and B , and W is the bandwidth in absence of diagonal disorder ($\Delta C=0$). $n_{A(B)}$ denotes the d -band occu-

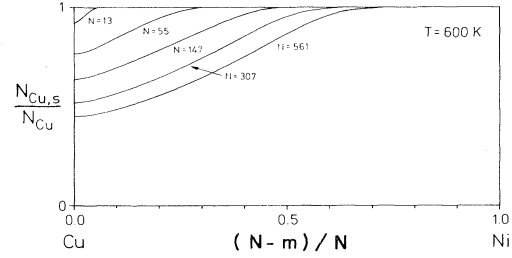


FIG. 5. Segregation behavior in small $\text{Cu}_{N-m}\text{Ni}_m$ clusters.

pancy of $A(B)$. In Fig. 5 we show results for the percentage of Cu atoms $N_{\text{Cu},s}/N_{\text{Cu}}$ effectively present at the surface of clusters with different size N as a function of their effective composition. (In this figure, it has been neglected that for small clusters x is discrete.) In Table II we also summarized the results for the equilibrium configuration of 55-atom large CuNi clusters with different total numbers of Cu and Ni atoms. In general, Eq. (2.13) must be extended to include strain effects which might influence the segregation behavior in the case of large differences in the atomic volumes of the alloy constituents.

E. Coulomb explosion of electrically charged clusters

In the following we attempt to calculate the stability of multiply charged small clusters.² For metallic and ionic clusters we assume that their Coulomb explosion consists of emitting charged single atoms at the surface of the cluster. Owing to the large cohesive energy this is the easiest way to reduce the Coulomb energy. Note also that metallic and ionic clusters are not easily deformable due to directional bonding. If $\delta E_{\text{Coul}}^{(n)}$ is the decrease in Coulomb energy due to emitting a singly charged surface atom with binding energy $E_{\text{coh},s}$ from an n -fold multiply charged cluster, then for $E_{\text{coh},s} \geq \delta E_{\text{Coul}}^{(n)}$ the cluster will be stable against emission of a charged atom.

In Fig. 6 results are given for the Coulomb energy $\delta E_{\text{Coul}}^{(n)}$ and the surface cohesive energy $E_{\text{coh},s}(N)$ for a doubly and threefold charged Pb cluster as a function of its size. The critical number of atoms $N_{\text{crit}}^{(n)}$, at which an n -fold multiply charged cluster becomes stable against emitting a positively charged atom, is calculated from

$$E_{\text{coh},s} = \delta E_{\text{Coul}}^{(n)}. \quad (2.14)$$

Note, we obtain from Fig. 6, using this formula, $N_{\text{crit}}^{(2)} \approx 28$, which compares very well with the experimental result² $N_{\text{crit}}^{(2)} = 30$. Furthermore, we find $N_{\text{crit}}^{(3)} \approx 130$.

The ratios of the critical numbers of atoms for which clusters explode are easily obtained as follows. For metal clusters the Coulomb energy consists of the (screened) interaction of the emitted pointlike charge with the perfectly conducting charged spherical cluster. In the case of doubly charged clusters the positive charge which is emitted from the surface and the center of gravity of the remaining cluster charge are separated by a distance $2\alpha r^{(2)}$ with $\alpha \gtrsim 1$. Then,

$$\delta E_{\text{Coul}}^{(2)} = \frac{e^2}{2\alpha r_{\text{crit}}^{(2)}} = E_{\text{coh},s}(N_{\text{crit}}^{(2)}). \quad (2.15a)$$

TABLE II. Equilibrium configuration in a $\text{Cu}_{N-m}\text{Ni}_m$ cluster with 55 atoms for different compositions.

Total composition		"Surface" composition		"Bulk" composition	
$N-m$ (Cu)	m (Ni)	N_s-m_s (Cu)	m_s (Ni)	N_b-m_b (Cu)	m_b (Ni)
0	55	0	42	0	13
5	50	5	37	0	13
10	45	10	32	0	13
15	40	15	27	0	13
20	35	20	22	0	13
25	30	25	17	0	13
30	25	30	12	0	13
35	20	35	7	0	13
40	15	40	2	0	13
45	10	42	0	3	10
50	5	42	0	8	5
55	0	42	0	13	0

Here, α includes screening of the charges. Similarly, for triply and quadruply charged clusters we obtain

$$\delta E_{\text{Coul}}^{(3)} = \frac{2e^2}{2\alpha' r_{\text{crit}}^{(3)}} = E_{\text{coh},s}(N_{\text{crit}}^{(3)}) \quad (2.15b)$$

and

$$\delta E_{\text{Coul}}^{(4)} = \frac{3e^2}{2\alpha'' r_{\text{crit}}^{(4)}} = E_{\text{coh},s}(N_{\text{crit}}^{(4)}) \quad (2.15c)$$

With the use of these expressions, the critical cluster size ratios $N_{\text{crit}}^{(2)}:N_{\text{crit}}^{(3)}:N_{\text{crit}}^{(4)}$ can be approximately determined by neglecting the size dependence of $E_{\text{coh},s}$ and assuming $\alpha \approx \alpha' \approx \alpha''$. Then,

$$r_{\text{crit}}^{(2)}:r_{\text{crit}}^{(3)}:r_{\text{crit}}^{(4)} = 1:2:3.$$

Finally, using $r \propto N^{1/3}$, we obtain

$$N_{\text{crit}}^{(2)}:N_{\text{crit}}^{(3)}:N_{\text{crit}}^{(4)} = 1:8:27. \quad (2.16)$$

This should provide a good estimate for not too small clusters. However, for smaller clusters the size dependence of $E_{\text{coh},s}$ must be included (see Fig. 6). Taking this into account we estimate for Pb clusters, assuming bulk bond lengths,

$$N_{\text{crit}}^{(2)}:N_{\text{crit}}^{(3)}:N_{\text{crit}}^{(4)} = 1:4:10.$$

This result seems to agree with preliminary experimental data.²²

In ionic clusters all charges are localized and at maximum distance, and no charge rearrangement is expected upon emission of a charged ion. Using similar arguments as in the case of metallic clusters we obtain

$$\delta E_{\text{Coul}}^{(2)} = \frac{e^2}{2r_{\text{crit}}^{(2)}} = E_{\text{coh},s}(N_{\text{crit}}^{(2)}), \quad (2.17a)$$

$$\delta E_{\text{Coul}}^{(3)} = \frac{2e^2}{\sqrt{3}r_{\text{crit}}^{(3)}} = E_{\text{coh},s}(N_{\text{crit}}^{(3)}), \quad (2.17b)$$

$$\delta E_{\text{Coul}}^{(4)} = \frac{3e^2}{4r_{\text{crit}}^{(4)}/\sqrt{6}} = E_{\text{coh},s}(N_{\text{crit}}^{(4)}). \quad (2.17c)$$

Using for simplicity again the approximation that the surface energy is independent of the cluster size, we obtain

$$r_{\text{crit}}^{(2)}:r_{\text{crit}}^{(3)}:r_{\text{crit}}^{(4)} = 1:2.3:3.7.$$

Thus for charged ionic clusters, one finds the estimate

$$N_{\text{crit}}^{(2)}:N_{\text{crit}}^{(3)}:N_{\text{crit}}^{(4)} = 1:12:49. \quad (2.18)$$

Note that also in the case of ionic clusters this ratio depends on the size dependence of $E_{\text{coh},s}$.

In contrast to metallic and ionic clusters an electron hole in a van der Waals cluster (such as Xe, CO₂, etc.) strengthens the bonds locally.² Hence the emission of single charged atoms is improbable. The Coulomb energy will rather transform into vibrational energy and the easily deformable clusters are likely to undergo a symmetric rupture into equal singly charged parts. Denoting the cohesive energy per unit area by γ and assuming again localized charges, we obtain from the stability criterion

$$\frac{e^2}{2r_{\text{crit}}^{(2)}} = \pi(r_{\text{crit}}^{(2)})^2\gamma, \quad (2.19a)$$

$$\frac{3e^2}{\sqrt{3}r_{\text{crit}}^{(3)}} = \frac{3}{2}\pi(r_{\text{crit}}^{(3)})^2\gamma, \quad (2.19b)$$

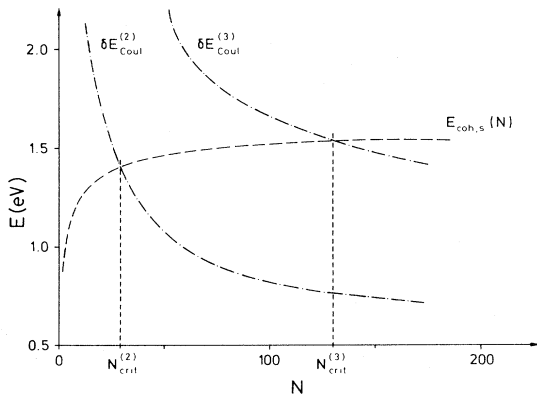


FIG. 6. Graphical determination of $N_{\text{crit}}^{(2)}$ and $N_{\text{crit}}^{(3)}$ for the Coulomb explosion in Pb. The change in Coulomb energy $\delta E_{\text{Coul}}^{(n)}$ is calculated by using Eq. (2.15) and assuming bulk bond lengths for determining r_{crit} from N_{crit} . The surface binding energy $E_{\text{coh},s}$ was obtained from Eq. (2.1).

and

$$\frac{6e^2}{4r_{\text{crit}}^{(4)}/\sqrt{6}} = 2\pi(r_{\text{crit}}^{(4)})^2\gamma \quad (2.19c)$$

for doubly, triply, and quadruply charged spherical clusters, respectively. Thus we obtain

$$N_{\text{crit}}^{(2)}:N_{\text{crit}}^{(3)}:N_{\text{crit}}^{(4)} = 1:2.3:3.7. \quad (2.20)$$

This compares well with the experimental result²² 1:2.4.

III. DISCUSSION

By comparison with experiment and with previous more elaborate calculations by Gordon *et al.*¹⁰ we conclude that the atomic and electronic structure of small clusters can be determined rather reliably using a fairly simple physical model. As shown in the Appendix our central Eq. (2.1) applies not only to transition metals, but approximately also to *s-p*-type metals such as Pb, etc. This encourages one to determine also magnetic²³ and catalytic properties^{13,14} of small clusters using a simplified physical picture.

It is likely that the binding energy of the most loosely bound atom in a cluster determines its stability. Clearly, if an $(N+1)$ -atom cluster lowers appreciably its energy by losing one atom, then in a cluster ensemble the population of clusters with $(N+1)$ atoms is much lower than the one for clusters with N atoms. It follows from Fig. 1(b) that clusters with the magic numbers $N=13, 19, 55, 79$, etc., atoms are most stable and should be observed in experiments producing clusters much more frequently than the others.¹ As physically expected, clusters with $N=13, \dots$ corresponding to the complete outermost shell are most stable. Note, for clusters with an incomplete outermost shell stability depends somewhat on the atomic arrangement in the surface shell. In our calculations clusters with an incomplete surface shell were generated by peeling off atoms one by one from opposite sides of the cluster such that the coordination of the most loosely bound atom is maximum. Note, an analogous yet more detailed treatment of incomplete surface-shell clusters with Lennard-Jones-type interatomic interactions was employed previously²⁴ in order to determine the equilibrium configuration and the cohesive energy. However, in contrast to our electronic calculation and also to experiment¹ these previous calculations yielded no magic numbers except for $N=13$. We expect on general grounds that the occurrence of magic numbers should differ for metallic- and van der Waals-type clusters, for example. Presumably for metallic clusters with relatively long-ranged interatomic interactions $E_{\text{coh},\text{min}}$ exhibits less pronounced jumps than might be the case for only short-ranged quasi-nearest-neighbor interactions in van der Waals-type clusters. Also for larger metallic clusters we expect $E_{\text{coh},\text{min}}$ to become smoother as a function of N .

Since the surface energy of close-packed structures such as fcc is lower than for bcc structures, for example, we expect for bulk bcc material a transition from fcc-like structures to bcc structure for increasing cluster size. Such a transition is illustrated in Fig. 3. Note, the calculations refer to clusters in equilibrium, which is significant since the energy differences involved are fairly small. Previous

calculations and also experiments²⁵ indicate that bulk electronic structure begins to occur for clusters with $N \geq 1000$ atoms, in agreement with our result shown in Fig. 3. Our result agrees also with the one for the corresponding icosahedra-cuboctahedra structural transition of clusters obtained by a somewhat more elaborate calculation.¹⁰ The critical cluster size N_{crit} (listed in Table I), at which the structural transition occurs for the bulk bcc metals, is determined by using numerical values of the structure energy ΔE_{bs} from Ref. 17, for which the hard-core effects have been neglected. Note that uncertainties in ΔE_{bs} and in the distance dependence of the hopping integrals (which determine a_{fcc} and a_{bcc}) can affect the critical cluster size N_{crit} considerably. To illustrate how N_{crit} depends on q (defined in the Appendix), we also used $q=5$ to determine N_{crit} for Cr. Using the corresponding values of a we obtain $N_{\text{crit}}(\text{Cr}) \approx 130$.

Furthermore, for calculating the structural stability we have neglected entropy contributions. Thus our results apply strictly only to clusters at zero temperature. Since we expect for the entropy $S \propto (T/\Theta_D)^3$ and for the cluster Debye temperature $\Theta_D^c = k\Theta_D^b$ [k being typically 0.6–0.9 for cluster sizes 30–60 Å (Ref. 26)], the entropy could play a role in determining the structural stability, if the change in Debye temperature for corresponding fcc and bcc clusters is large enough.

As shown in Fig. 4 we obtain a much larger average bond contraction than obtained assuming a uniform cluster relaxation.¹⁰ This results from the fact that even for small bond contractions the gain in relaxation energy at the surface is compensated by the loss in cohesive energy in the bulk of a uniformly contracted cluster, especially for larger cluster sizes. Our results agree reasonably well with experimental values. However, since experimental results are scarce presently, it is not possible to conclude definitely that contraction of small clusters occurs essentially at their surface as is expected for larger clusters, in analogy to surface contraction of bulk material. From experimental results by Apai *et al.*⁶ it was concluded that the bond contraction is proportional to the inverse cluster diameter d . This follows also from our analysis yielding that the bond contraction is proportional to the dispersion $D \equiv N_s/N \propto d^{-1}$. Note, our calculations neglect electronic configurational changes, $s \rightleftharpoons d$, which might occur at the surface. Furthermore, one expects the cluster contraction to vary for different metals, for example, throughout the transition-metal series. Such a possible variation is indicated in Fig. 4 where results are given for different p, q values which might be assigned to different transition metals, for example. In analogy to the discussion presented for the electron-phonon interaction in transition metals²⁷ one may argue that the contraction is determined by the change in the d -electron hopping integral Δt , which depends on the transition-metal valence. Further experimental studies of cluster contraction are needed for conclusive comparison with theoretical results. In particular, it would be interesting to study Invar alloys such as $\text{Ni}_{1-x}\text{Fe}_x$ and the effect of cluster contraction on alloy formation.

In calculating the cohesive energy and the structural stability we have neglected the change in energy due to relaxation. However, this change in energy is typically 1% of the cohesive energy. Also, as the difference in relaxa-

tion energy for small fcc and bcc clusters is about 0.5% of their cohesive energy, the influence of relaxation can also be neglected for the calculation of the structural stability.

Alloy formation of clusters is obviously of considerable interest. Note, if N_s and N are of the same order, then the surface segregation controls the alloy formation. To shed light on this problem, we studied in Fig. 5 segregation in small clusters. Drastic demixing might occur in small alloy clusters since N is finite, and consequently, the concentration of A changes appreciably in the center of the cluster when A atoms segregate to the cluster surface. This is illustrated in Fig. 5 and Table II. The significance of the cluster size for segregation, especially in small alloy particles (Fig. 5), has been discussed by Helms²⁰ previously. Note in Fig. 5 that in the extreme case of infinitely large $\text{Cu}_{N-m}\text{Ni}_m$ clusters the value $N_{\text{Cu},s}/N_{\text{Cu}}$ approaches zero, because for a given concentration it is proportional to the fraction of surface atoms in the cluster. The decrease of $\Delta E(N)$ for decreasing cluster size lowers segregation. The cluster contraction favors demixing if the alloy atoms differ in atomic volume. The segregation behavior of alloy clusters for decreasing cluster size, illustrated in Fig. 5 for the case of $\text{Cu}_{1-x}\text{Ni}_x$ alloys, might also explain the self-purification effect observed recently for Li clusters containing Na impurities.²³ Note, segregation in small fcc clusters changes when the structural transition to bcc structure occurs.

The stability of electrically charged clusters is a very important problem of relevance in different areas of physics. We have shown [see Fig. 6 and Eqs. (2.15), (2.17), and (2.19)] that the Coulomb explosion of clusters depends sensitively on the cohesive force and can be explained by using a simple physical model. Our results for the critical cluster size agree excellently with recent experimental results.² Of course, the Coulomb explosion of clusters, in particular metallic ones, should somewhat depend on the surface structure of the cluster, as charged atoms at edges and corners are expected to fall off more easily. Note, applying the expression for $E_{\text{coh},s}$, Eq. (2.1), to Pb yields very good agreement with experiment. As expected, our criterion for the Coulomb explosion, Eq. (2.14), yields results for the stability of charged A_3^{2+} trimers which agree well with experiment.²⁸ Thus, for example, we find that Ni_3^{2+} is stable, while Ni_2^{2+} is unstable. It is interesting to note that one obtains empirically²⁸ $\delta E_{\text{Coul}}^{(2)} = 1.3E_{\text{coh}}^d$, where $\delta E_{\text{Coul}}^{(2)}$ denotes the bare Coulomb interaction energy between the two charges and E_{coh}^d the binding energy of a dimer. On the basis of our calculation we conclude that the factor 1.3 in the above relationship arises mainly from neglecting the screening of the charges and the binding of the emitted atom from its NNN in the trimer molecule.

Small clusters should exhibit interesting behavior with regard to many other properties, e.g., metal-insulator transitions. Owing to the change in coordination number such transitions might be observable in small Hg, Rb, and Cs clusters as a function of cluster size in analogy to the Mott transition in expanded Hg and to the Hubbard transition in expanded Cs and Rb. For example, in expanded Hg vapor this transition occurs at a density $\rho \approx 8-9 \text{ g/cm}^3$, corresponding to an effective coordination²⁹ of about 6-7. Thus, we may estimate that this transition occurs in clusters with $20 \leq N_{\text{crit}} \leq 50$ atoms. This seems to be confirmed by recent experimental results.³⁰ Also the metal-

insulator transition observed for bulk liquid $\text{Cs}_x\text{Au}_{1-x}$ alloys might change drastically for corresponding small clusters due to the alloy demixing discussed earlier in this paper.

In summary, we have demonstrated that some important properties of small (metallic) clusters can be understood even quantitatively in terms of a simple physical model, permitting easy calculations.

ACKNOWLEDGMENTS

We acknowledge useful discussions with Professor E. Recknagel, Professor F. Hensel, Dr. K. Sattler, and Dr. D. G. Pettifor. One of us (S.M.) acknowledges financial support from the Deutsche Forschungsgemeinschaft (Sonderforschungsbereich 6).

APPENDIX

In the following we derive the cohesive energy formulas used throughout the paper. Assuming a hard-core repulsion, the binding energy of the atom i at equilibrium configuration in a metallic cluster is approximately given by³¹

$$E_{\text{coh}}(i) = - \sum_{\alpha} \int_{-\infty}^{E_F} dE (E - E_0^{\alpha}) N_i^{\alpha}(E). \quad (\text{A1})$$

Here, the summation extends over all partly occupied bands α , $N_i^{\alpha}(E)$ is the local density of states, and E_0^{α} the α -band center at site i . E_F is the Fermi energy of the system. While this linear combination of atomic orbitals (LCAO) formula has been mainly used to describe cohesion in d metals, the formalism also applies to s - p metals,³² provided also the second- and third-nearest-neighbor interactions are considered in calculating $N_i^{\alpha}(E)$.

This formula can easily be evaluated, if a rectangular band shape is assumed for $N_i(E)$. Then, assuming for simplicity only one band,

$$E_{\text{coh}}(i) = \frac{W_i}{2L} n_i (L - n_i), \quad (\text{A2})$$

where $L = 2(2l + 1)$, $l = 0, 1, \dots$, is the maximum and n_i the effective band occupancy, and W_i is the local bandwidth.

A still more general formula can be obtained from (A1) by using the fact that $E_{\text{coh}}(i)$ is proportional to a factor changing the energy scale. Then, while all local band occupancies n_i and the band shapes remain constant, each term in the sum in (A1) is proportional to the bandwidth W_i^{α} . Depending on the band shape (rectangular or more realistic), W_i^{α} is proportional to the square root of the second moment $M_{2,i}^{\alpha}$ of $N_i^{\alpha}(E)$, which is given by

$$M_{2,i}^{\alpha} = \int_{-\infty}^{+\infty} dE (E - E_0^{\alpha})^2 N_i^{\alpha}(E). \quad (\text{A3})$$

In the LCAO formalism one obtains³¹

$$M_{2,i}^{\alpha} = \sum_j' (t_{ij}^{\alpha})^2, \quad (\text{A4})$$

where t_{ij} denotes the intersite hopping integral and the sum extends over all neighbors of i . Distinguishing the first, second, etc., neighbors, one can write

$$\begin{aligned} M_{2,i}^{\alpha} &= Z_i^1 (t_1^{\alpha})^2 + Z_i^2 (t_2^{\alpha})^2 + \dots \\ &= (t_1^{\alpha})^2 (Z_i^1 + aZ_i^2 + \dots), \end{aligned} \quad (\text{A5})$$

where the quantity $Z_i^1 + aZ_i^2 + \dots$ is the effective coordi-

nation Z_i . For constant interatomic distances the α band-width W_i^α , and hence each term of the sum in (A1), is proportional to $(Z_i)^{1/2}$, if the local electronic configuration (total number and s - p - d distribution of the valence electrons) is assumed to be the same as in the bulk and changes in the band shape can be neglected. Then,

$$E_{\text{coh}}(i) = (Z_i/Z_b)^{1/2} E_{\text{coh}}(\text{bulk}). \quad (\text{A6})$$

These two conditions seem to apply especially well to transition metals near the noble-metal end, such as Ni, Cu, Ag, and Au. Even for dimers of such elements the cohesive energy calculated from (A6) by using bulk data¹⁸ agrees within 5% with experimental results.³³ The applicability of Eq. (A6) to Pb, etc., is well demonstrated by the

agreement found for the atomization energy of Pb_2 (theoretical, 1.17 eV; experimental,³⁴ 0.84 eV), Pb_3 (theoretical, 2.47 eV; experimental,³⁴ 2.32 eV), and Pb_4 (theoretical, 4.04 eV; experimental,³⁴ 4.23 eV), if the bulk cohesive energy³³ of Pb, 2.02 eV, is used.

Often small changes in E_{coh} due to relaxation in the interatomic distances are of interest (e.g., in order to determine the equilibrium geometry). Then, the distance dependence of the binding and the repulsive part of E_{coh} must be considered. The binding part can easily be obtained along the lines presented above, by using a one-band model. The repulsive part is given by a Born-Mayer potential, which shows an exponential distance dependence, in analogy to the hopping integrals. Then,³⁵

$$E_{\text{coh}}(i) = \frac{E_{\text{coh}}(\text{bulk})}{(1-q/p)(Z_{\text{bulk}})^{1/2}} \left[\left(\sum_j e^{[-2q(R_j/R_0-1)]} \right)^{1/2} - \frac{1}{(Z_i)^{1/2}} \frac{q}{p} \sum_j e^{[-p(R_j/R_0-1)]} \right], \quad (\text{A7})$$

where R_j and R_0 denote the relaxed and the bulk nearest-neighbor distance, respectively. For the parameters p and q the values $p \approx 9$ and $q \approx 3$ have been proposed for transition metals.³⁵ Note, Eq. (A7) has been used previously to calculate the relaxation at low-index single-crystal transition-metal surfaces.³⁵ With the use of $q=3$ for the distance dependence of the hopping integral in (A7), one

easily obtains $a=0.08$ ($a=0.4$) for a fcc (bcc) lattice in (A5). It emerges from Eq. (A7) that the gain in binding energy of an average atom upon structure relaxation (of typically $\leq 5\%$) is less than 1% of the average cohesive energy. Hence the negligence of cluster relaxations in Eq. (A6) has no effect on the cohesive energy.

*Permanent address: Freie Universität Berlin, Arnimallee 14, D-1000 Berlin 33, West Germany.

¹O. Eht, K. Sattler, and E. Recknagel, Phys. Rev. Lett. **47**, 1121 (1981).

²K. Sattler, J. Mühlbach, O. Eht, and E. Recknagel, Phys. Rev. Lett. **47**, 160 (1981).

³A. Schmidt-Ott, P. Schurtenberger, and H. C. Siegmann, Phys. Rev. Lett. **45**, 1284 (1980).

⁴Yu. F. Komnik, Fiz. Tverd. Tela (Leningrad) **10**, 312 (1968) [Sov. Phys.—Solid State **10**, 2483 (1968)]; N. T. Gladkikh and V. N. Khotevich, Ukr. Fiz. J. **16**, 1429 (1971).

⁵A. Renou and M. Gillet, Surf. Sci. **106**, 27 (1981).

⁶G. Apai, J. F. Hamilton, J. Stöhr, and A. Thompson, Phys. Rev. Lett. **43**, 165 (1979).

⁷B. Moraveck, G. Clugnet, and J. Renoupeuz, Surf. Sci. **81**, L631 (1979).

⁸R. P. Messmer, S. K. Knudson, K. H. Johnson, J. B. Diamond, and C. Y. Yang, Phys. Rev. B **13**, 1396 (1976); R. P. Messmer, Surf. Sci. **106**, 225 (1981).

⁹R. C. Baetzold, M. G. Mason, and J. F. Hamilton, J. Chem. Phys. **72**, 366 (1980); R. C. Baetzold, Surf. Sci. **106**, 243 (1981).

¹⁰M. B. Gordon, F. Cyrot-Lackmann, and M. C. Desjonquères, Surf. Sci. **80**, 159 (1979).

¹¹J. Demuyck, M. M. Rohmer, A. Strich, and A. Veillard, J. Chem. Phys. **75**, 3443 (1981).

¹²I. D. Monokhov, V. I. Petinov, L. I. Trusov, and V. F. Petrunin, Usp. Fiz. Nauk. **133**, 653 (1981) [Sov. Phys.—Usp. **24**, 295 (1981)].

¹³J. R. Anderson, *Structure of Metallic Catalysts* (Academic, London, 1975).

¹⁴J. H. Sinfelt, Rev. Mod. Phys. **51**, 569 (1979), and references cited therein.

¹⁵Note, for small clusters icosahedra structure is more stable than fcc structure (Ref. 10), which has nearly the same packing of atoms. By using Eq. (2.1) for calculating cohesion one is of course not able to describe the fine differences between the electronic structures of fcc and icosahedra clusters. For simplicity we use fcc-type clusters.

¹⁶J. P. Borel, Surf. Sci. **106**, 1 (1981).

¹⁷D. G. Pettifor, J. Phys. C **3**, 367 (1970).

¹⁸R. Hultgren, P. D. Desai, D. T. Hawkins, M. Gleiser, K. K. Kelly, and D. D. Wagman, *Selected Values of the Thermodynamic Properties of the Elements* (American Society of Metals, Cleveland, 1973).

¹⁹A. Tamura, K. Higet, and T. Ichinokawa, J. Phys. C **15**, 4975 (1982).

²⁰C. R. Helms, in *Interfacial Segregation*, edited by W. C. Johnson and J. M. Blakely (American Society of Metals, Cleveland, 1979), p. 175.

²¹Ph. Lambin and J. P. Gaspard, J. Phys. F **10**, 2413 (1980).

²²K. Sattler, in Proceedings of the Thirteenth International Symposium on Rarefied Gas Dynamics, USSR, Novosibirsk, July 1982 (unpublished), and private communication.

²³P. E. Chizhov, V. I. Petinov, and A. V. Grigorevski, Solid State Commun. **42**, 327 (1982).

²⁴M. R. Hoare and P. Pal, Adv. Phys. **20**, 161 (1971); **24**, 645 (1975).

²⁵M. Grunze, Chem. Phys. Lett. **58**, 409 (1978).

²⁶G. H. Comsa, D. Heitkamp, and H. S. Råde, Solid State Commun. **24**, 547 (1977).

²⁷S. Barišić, J. Labbé, and J. Friedel, Phys. Rev. Lett. **25**, 919 (1970).

²⁸Th. Jentsch, W. Drachsel, and J. H. Block, Chem. Phys. Lett. **93**, 144 (1982).

²⁹F. Hensel, in *Liquid and Amorphous Metals*, edited by E.

- Lüscher and H. Coufal (Sijthoff and Noordhoff, Amsterdam, 1979).
- ³⁰F. Hensel (private communication).
- ³¹J. Friedel, in *The Physics of Metals I Electrons*, edited by J. M. Ziman (Cambridge University Press, London, 1969).
- ³²W. Y. Ching and J. Callaway, *Phys. Rev. B* 11, 1324 (1975).
- ³³*CRC Handbook of Chemistry and Physics*, edited by R. C. Weast (CRC, Cleveland, 1974), Vol. 55.
- ³⁴K. A. Gingerich, D. L. Cocke, and F. Miller, *J. Chem. Phys.* 64, 4027 (1976).
- ³⁵R. P. Gupta, *Phys. Rev. B* 23, 6265 (1981), and references cited therein.

Errata

**Erratum: Hot luminescence in *trans*-polyacetylene: A picosecond time-resolved study
[Phys. Rev. B 27, 6545 (1983)]**

John R. Andrews, T. E. Orlowski, Harry Gibson, Michael L. Slade,
Wayne Knox, and Bruce Wittmershaus

Bruce Wittmershaus is the correct spelling of the final author's name.

**Erratum: Simple theory for the electronic and atomic structure
of small clusters
[Phys. Rev. B 28, 665 (1983)]**

D. Tománek, S. Mukherjee, and K. H. Bennemann

Please note that in Eqs. (2.8) and (A7) Z_i should be replaced by Z_{bulk} . The results shown in the paper are obtained by using the correct equations.

**Erratum: Adams representation and localization in a magnetic field
[Phys. Rev. B 28, 811 (1983)]**

I. Dana and J. Zak

The matrix elements of Q and P [Eq. (24)] should be replaced by the following expressions:

$$\langle l\vec{\kappa} | Q | l'\vec{\kappa}' \rangle = \left[i \frac{\partial}{\partial \kappa_2} \delta_{ll'} + i Z_{ll'}^{(2)}(\vec{\kappa}) \right] \hat{\Delta}(\vec{\kappa} - \vec{\kappa}') ,$$

$$\langle l\vec{\kappa} | P | l'\vec{\kappa}' \rangle = \left[\frac{\beta}{i} \frac{\partial}{\partial \kappa_1} \delta_{ll'} + \hbar \kappa_2 + \frac{\beta}{i} Z_{ll'}^{(1)}(\vec{\kappa}) \right] \hat{\Delta}(\vec{\kappa} - \vec{\kappa}') ,$$

$$Z_{ll'}^{(j)}(\vec{\kappa}) = \int d\bar{P} \varphi_{l\vec{\kappa}}^*(\bar{P}) \frac{\partial}{\partial \kappa_j} \varphi_{l'\vec{\kappa}'}(\bar{P}), \quad j=1, 2 .$$

Thus, these matrix elements are, in general, not diagonal in the magnetic band index, and they do depend on the detailed magnetic band structure through the quantity $Z_{ll'}^{(j)}(\vec{\kappa})$. The claim in the manuscript that the orbital (36) with (45) assumes the minimal undeterminacy $\Delta x_0 \Delta y_0$ is generally not correct.